COMPREHENSIVE NUMERICAL MODEL FOR THE ANALYSIS OF POTENTIAL HEAT RECOVERY SOLUTIONS IN A CERAMIC INDUSTRY

M. Venturelli[1], D Brough[2], M. Milani[1], L. Montorsi[1], Hussam Jouhara[2]

1. Department of Sciences and Methods for Engineering, University of Modena and Reggio Emilia, Reggio Emilia, Italy
2. College of Engineering, Design and Physical Sciences, Brunel University London, Uxbridge, Middlesex, UB8 3PH, London, UK.

ABSTRACT

Heat recovery opportunities and total plant energy efficiency improvements need to be evaluated before manufacturing the real components when addressing the energy and economic effectiveness in industrial applications.

Numerical modelling of the complete energy systems can be a key design tool in order to investigate the potential solutions to improve the performance of the considered system.

In this study, a 0D/1D numerical analysis is adopted to investigate the energy efficiency enhancement given by the application of a heat pipe based heat exchanger in a ceramic industry; the thermal power is recovered from the exhaust gases of the kilns used to fire the tiles.

The numerical model includes all the main components of the heat recovery system: the primary side of the exhaust gases, the heat exchanger, the secondary circuit of the heat transfer fluid and the heat sink where the thermal power is exploited.

Particular care is devoted to the modelling of the heat pipe based heat exchanger and the control strategy of the system; a specific model for the simulation of the secondary side pump is also accounted for in the analysis.

The numerical results of the primary circuit are validated against experimental measurements carried out on the real ceramic facility.

The good agreement between the numerical and experimental results demonstrates that the numerical model is an appropriate tool for investigating the energy efficiency enhancement of an industrial plant and for evaluating different configurations and solutions in order to fulfil the industry requirements.

Keywords: Numerical Model, Heat Recovery, Energy efficiency, Ceramic industry, environmental impact.

1 Introduction

The application of waste heat recovery systems in the industrial contexts has recently attracted considerable interest due to the increasing consciousness of the impact of global warming in transforming our environment and due to the constant increase in fuel prices [1].

Thus, the waste heat recovery from exhaust streams is one of the key factors to be competitive for businesses in a continuously changing marketplace.

Within this context, the ceramic industry can be considered suitable for this kind of application because it is characterized by energy intense processes and a huge amount of waste heat is conveyed to the atmosphere; indeed, it has been estimated that only the Italian ceramic tile and refractory materials industry has a consumption of gas methane equal to 1.5 billion cubic meter per year and by an electricity demand of 1800 GWh/y [2]. Thus, the energy efficiency of the ceramic process can be improved by the waste heat recovery determining a reduction in the greenhouse gases emission and in the primary energy cost.

In literature, Jouhara at al. [3] studied the application of the waste heat recovery systems in the iron and steel, food and ceramic industry; a comprehensive review of waste heat recovery methodologies was presented, and the advantages and disadvantages of the main techniques were evaluated. An accurate analysis of the waste heat technologies that can be applied to the aluminium industry was carried out in [4].
In the ceramic sector, different solutions for the waste heat recovery from exhaust sources have been analysed and several measures and techniques that can be implemented in order to enhance the energy efficiency of the tile manufacturing process were reviewed in the report named "Reference Document in the Ceramic Manufacturing Industry" [5]. One of the most practised technique mentioned in [5] is the heat recovery from the excess air of the furnace; the hot air recovered from the cooling zone of the roller kiln can be used for heating up the air for the drying stage. A theoretical approach for the evaluation of the energy recovery due to the exploitation of the cooling gases in the exhaust chamber was presented in [6]; the study quantified a saving of the 17 %.
The second strategy to enhance the energy efficiency of the process is the installation of cogeneration units due to the simultaneous demand of heat and electric power required for the industrial process [7]. Organic Rankine Cycle have been also adopted and applied to the ceramic process; for instance, in [8] an ORC-system was used to recover heat from the indirect cooling section of the kiln to produce electricity. The analysis demonstrated that it is possible to recover thermal power from 128.19 kW to 179.87 kW while the maximum electrical power is ranged between 21 kW and 18.51 kW.
The accurate prediction of the waste heat recovery system performance is fundamental for the solution optimization and integration in the existing industrial process and for the evaluation of the economics of the design. Nevertheless, the design of waste heat recovery systems can be improved by adopting numerical tools for the evaluation of different solutions and configurations and for the investigation of the performance before manufacturing the real system or modifying an existing plant [9].
Furthermore, the numerical analysis can be exploited to study the system behaviour under time dependent operating conditions or under critical situations that could potentially occur.
In literature, there are many examples that a numerical approach for the simulation of thermo-hydraulic components or energy system in general.
For instance, in [10] a numerical approach was adopted for the investigation of the evolution of the temperature distribution and the thermo-mechanical stresses due to a liquid aluminium injection through a nozzle for a cogeneration system based on Al-H_2O reaction.
In the field of industrial food processing, a numerical approach has been adopted to investigate the operating parameters of the fruit and vegetables drying process [11]. Bunyawanichakul et al. [12] investigated a pneumatic dryer plant for rice processing where heat and mass transfer has been modelled with a 0D/1D approach. Similarly, a 0D/1D steady state approach was used to analyse different thermal configurations of thermoelectric generator for HVAC [13]. Luo Y. et al [14] carried out a steady state numerical analysis for determining the energy efficiency enhancement obtained by the combined use of PV façade and solar cooling. The performance of a lab-scale heat pipe based heat exchanger was investigated in [15] comparing the results of an experimental campaign with the calculations obtained by means of a transient numerical simulation model; a good agreement was demonstrated and the study predicted 33 months payback for a theoretical full scale unit.
In [16] the heat recovery system for the post combustion flue gas treatment in a coffee roaster plant is investigated using a lumped and distributed parameter numerical modelling.
In the field of the ceramic industry, Milani et al. developed a lumped and distributed parameter numerical model of an entire ceramic kiln to simulate the performance of the system under actual operating conditions [9]. Similarly, in [17] a combined theoretical and numerical approach was adopted in order to determine the thermal energy that can be recovered by the application of a heat pipe based heat exchanger to the cooling stack of the ceramic kiln. It was demonstrated that a reduction of approximately 110600 Sm^3 per year of natural gas can be saved determining a reduction of 164 tonnes per year of carbon dioxide.

An additional study related to the ceramic sector was conducted by Gomez et al. [18]; the study numerically investigated the feasibility of the natural gas substitution by syngas in ceramic furnaces. The numerical simulations, in this case computational fluid dynamic approach, were used to determine the proper geometry for the syngas burner.
Modelling and multi-criteria optimization was used in [19] to simulate and optimize the application of a combined heat and power generation system to a tile manufacturing industrial process. The optimization process was carried out considering energy, economic and environmental variables in the objective function; the designed parameters of the systems (number and capacity of the prime movers, heating capacity of the boiler and cooling capacity of the chiller) were determined with the numerical model. Finally, the numerical analysis has been adopted in [20] to investigate the thermal and fluid dynamic behaviour of a ceramic tile cooking roller kiln and combined with the analysis of the mechanical stresses formed in the final ceramic product. The 0D/1D model has been employed to determine the influence of the cooling temperature profile on the final residual stresses of the tiles. The study demonstrated that the ideal cooking profile can be obtained in the real kiln by varying the operating parameters to obtain an improvement of the quality of the tiles.
This paper is part of the Horizon 2020 project – ETEKINA (heat pipe technology for industrial applications) (www.etekina.eu). In this project, the goal is to recover the 40 % of the waste heat contained in the exhaust streams of three different industrial contexts (aluminium, steel and ceramic sector) and to re-use the recovered thermal energy in the industrial processes in order to decrease their carbon emissions [1].
This paper focuses on the ceramic industry and it investigates the application of an heat pipe based heat exchanger to a ceramic plant; the benefits gained by the HPHE installation in terms of energy efficiency improvement and in terms of environmental impact reduction of the ceramic process are determined by means of a lumped and distributed numerical modelling.
The 0D/1D model includes the entire heat recovery system which consists of the primary and secondary circuit. In particular, the primary side of the system is composed by the waste heat source that is the exhaust gases of two ceramic furnaces. The heat recovery unit, i.e. HPHE, is considered in the model to simulate the thermal power recovered to the heat transfer fluid, which is the secondary stream of the circuit modelled. Water is pumped in the secondary circuit as heat transfer fluid; the numerical model of the secondary side accounts for a specific model for the simulation of the pump and for the heat sink where the thermal power recovered is exploited.
Experimental data (temperatures and flow rate of the primary side) are used as boundary conditions for the simulation of the heat recovery system performance to assess the stability of the designed control strategy of the system.
The numerical results related to the thermal losses along the exhaust piping are validated against experimental data while the thermal performance of the entire heat recovery system numerical model is validated against theoretical correlations under nominal conditions.
Finally, the adoption of the heat pipe based heat exchanger in order to recover the heat from the exhaust gases of the tile firing process of two ceramic furnaces reduced the fuel consumption of approximately the 40 % with the respect to the system in its current layout, i.e. without heat recovery, and the simulation demonstrated that the designed control strategy is reliable in order to keep the operating parameters in the desired range.
Indeed, the 0D/1D model will be used to investigate the fluid dynamic behaviour of the entire heat recovery system and it will enable to perform simulations for testing the influence of the control strategy parameters on the thermal performance of the heat recovery system.
Thus, the testing of different control strategies parameters when different phenomena could take place including the excess or the decrease of thermal energy available in the exhaust and the decrease of thermal energy required by the heat sink process is performed in a reasonable time and with acceptable computational effort.

Therefore, the 0D/1D model is a valuable tool for the tuning the control strategy and for tailoring its parameter to maintain the desired working conditions of the system reducing remarkably time and costs; indeed, the simulations gives the opportunity to investigate different working points of the system that, otherwise, would have analysed by experimental tests.

2 Test case

The heat recovery closed loop circuit simulated in this study is a system that will be installed within the Etekina project in a real ceramic tile production facility located in the ceramic district in Emilia Romagna, Italy.

The ceramic process is an energy intensive production system characterized by significant consumption of electric energy and natural gas.

The ceramic process starts with a selection of the raw materials (mainly clays, feldspars, sands, kaolin) and they are grinded in continuous mills with a mixture of water. Secondly, hydraulic presses are used to mechanically compress the paste in order to create ceramic ware with a regular geometry; the tile body are then dried in order to reduce the water content, they are decorated and finally fired in ceramic furnaces at approximately 1250 °C.

Focusing on the thermal energy consumption of the ceramic process, the firing stage is responsible for approximately the 53 % of thermal consumption, followed by the spray drying (35%) and drying (10 %) [21].

In Etekina project, the exhaust gases of two firing furnaces have been selected to be addressed as the heat source for the waste heat recovery since they are a potential source of high specific enthalpy and they are characterized by interesting temperatures and flows (220-250 °C, 10000-15000 Nm^3/h per kiln).

Thus, an heat pipe based heat exchanger will be installed in the ceramic facility before the main stack and the recovered heat from the flue gases of the furnaces will be transferred via a thermo-vector fluid, i.e. water, to the spray dryer; the heat recovered by the water will be transferred to the air used in the spray dryer by means of two intermediate heat exchangers positioned in parallel. This heat recovery reduces the spray dryer natural gas consumption of approximately the 40 %.

Figure 1 shows the sketch of the of the heat recovery system layout representing the main designed operating parameters: in a regime working cycle, the exhaust gases are cooled down from the temperature of 245 °C at the inlet of the HPHE to approximately 155 °C, i.e. at the outlet of the heat exchanger; in the secondary side, the heat transfer fluid will benefit of approximately 50 °C of delta temperature, since the designed temperature at the inlet of the system is 115 °C while at outlet of the system is 165 °C.

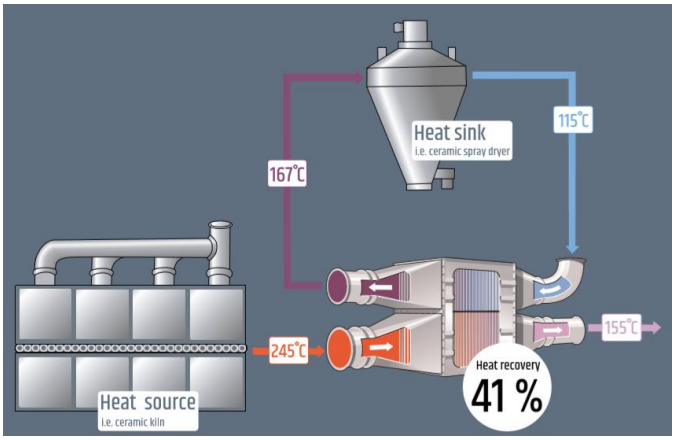

Figure 1: Sketch of the designed heat recovery system

In the real facility, the existing primary side, i.e. the exhaust circuit, is equipped with different sensors that monitor the main operating parameters, i.e. temperatures, pressures, and flow rates.

The sensors provided a time history of the monitored quantities sampling on 15 minute-basis; the sensors installed are listed in Table 1 while their locations are shown in Figure 2.

As shown from the Figures, the sensors provide a complete characterization of the fluid dynamic behaviour of the exhaust gases; indeed, different thermocouples are installed along the piping in order to monitor the thermal losses in the main section of the pipeline and across the main component, i.e. filter.

In the designed heat recovery configuration, the HPHE will be installed before the filter to increase the temperature of the exhaust gases at the inlet of the system.

A detailed control strategy has been designed to keep under control the main operating parameters of the heat recovery system: the outlets' temperatures at the HPHE, i.e. temperature of the exhaust gases (primary side) and temperature of the water (secondary side), which are respectively 155 °C and 165 °C. In particular, the heat transfer fluid circuit is equipped with a pump and an inverter in order to vary the flow rate of the water fluid; the desired temperatures at the outlets of the heat exchanger are maintained by varying the speed of the pump.

If the thermal power available in the exhaust gases exceeds the designed value and the higher flow rate in the secondary circuit, due to the increased speed of the pump, is not enough in order to keep the temperatures in the desired range, a bypass valve is partially opened; this level of the control strategy enables to decrease the thermal power available in the exhaust gases.

A total bypass of the HPHE primary side will be operated during downtime periods of the heat sink and during maintenance procedures.

On the opposite, when the exhaust energy content is lower than the nominal value, the pump decelerates; if the minimum rotational speed of the pump is not sufficient to maintain the water temperature at 165 °C, the bypass of one of the intermediate heat exchangers will be generated in order to decrease the thermal power exploited in the spray-dryer.

Thus, the temperatures at the outlet of the HPHE will increase.

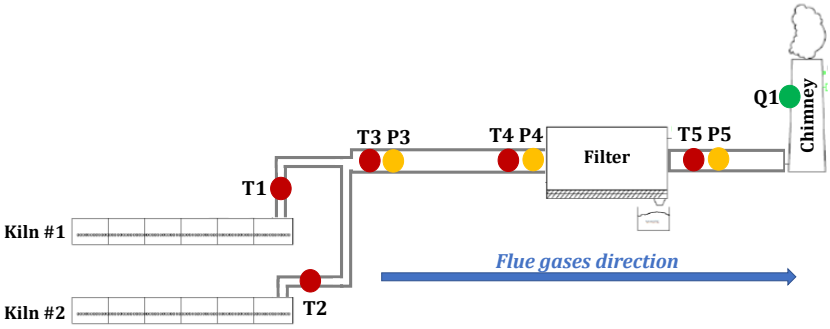

Figure 2: Location of the sensors installed along the exhaust piping in the real facility

Table 1. Specification of the sensors installed

Type of Sensor	Location	Reference letter
Temperature transducer	Beginning of the exhaust piping of the Kiln#1	T1
Temperature transducer	Beginning of the exhaust piping of the kiln#2	T2
Temperature transducer	Manifold	T3
Pressure Transducer	Manifold	P3
Temperature transducer	Filter INLET	T4
Pressure Transducer	Filter INLET	P4
Temperature transducer	Filter OUTLET	T5
Pressure Transducer	Filter OUTLET	P5
Pitot Tube	Exhaust stack outlet	Q1

This study focuses particularly on the development of a 0D/1D numerical model for the simulation of the entire heat recovery system. Firstly, the numerical model of the primary side is developed for the simulation of the heat losses along the exhaust piping; the numerical results are compared and validated against experimental data available from the sensors.
The lumped and distributed analysis is then improved with the introduction of specific models for the heat pipe based heat exchanger and the secondary circuit of the heat transfer fluid; the numerical model is validated against theoretical correlations used to design the system. Table 2 lists the main operating parameters of the designed heat recovery system
Finally, the numerical modelling is used to study the effects of the waste heat recovery and the response of the control strategy to working conditions that could occur in the real system; the time dependent simulations determine the working points of the heat recovery system for the tuning of the control strategy.

Table 2. Operating parameters of the designed heat recovery system

Designed Parameters	Quantity
Exhaust Temperature HPHE INLET	245 °C
Exhaust Temperature HPHE OUTLET	155 °C
Water Temperature HPHE INLET	115 °C
Water Temperature HPHE OUTLET	165 °C
Thermal Power Recovered	700 kW

3 Materials and methods

3.1 HPHE Numerical Model

TRNSYS Numerical Model (Dan)

3.2 Heat Recovery System Numerical Model

(Matteo)

The numerical model of the entire heat recovery system simulated in this study is developed by means of the software LMS Imagine.Lab AMEsim, licensed by Siemens [22].

The heat recovery system includes three main sections: the exhaust circuit (primary side), the heat pipe-based heat exchanger and the heat transfer fluid circuit (secondary side). The numerical model accounts for the pneumatic and thermal hydraulic libraries for the simulation of the flue gases and water circuit respectively; in addition, the thermal library has been used to consider the solid parts of the circuits and their influence on the whole heat exchange.

The numerical model simulates the exhaust flow inside the primary piping accounting for the thermodynamic properties of the considered gas and the semi-perfect gases approach is accounted in the simulation. The numerical model of the exhaust circuit simulates the flue gases from the outlets of the two ceramic kilns to the main stack; the input parameters are the flow rate and temperature of the gases measured by the sensors installed along the piping.

The heat recovery from the exhaust gases is transferred to the water flow by means of an heat exchanger located before the main stack; the waste heat recovery system is based on the heat pipe technology which uses the two-phase cycle (boiling and condensation) of a working fluid in order to transfer the heat from the hot stream to the cold one.

Due to the fact that the “two-phase flow” library is not fully developed, the system has been modelled considering the heat pipes walls as superconductors. Thus, a high value for the thermal conductivities of the evaporator and condenser sections of the heat pipes have been implemented in the software to account for the evaporation and condensation phenomena respectively.

Commentato [LM1]: This part has To be reworked on the basis of the TRNSYS results.

The water of the secondary side is simulated with a thermal-hydraulic library and the fluid properties (density, specific heat, dynamic viscosity, thermal conductivity) are modelled by polynomials of the pressure and temperature.

The following Figure shows the layout of the numerical model implemented in AMESim.

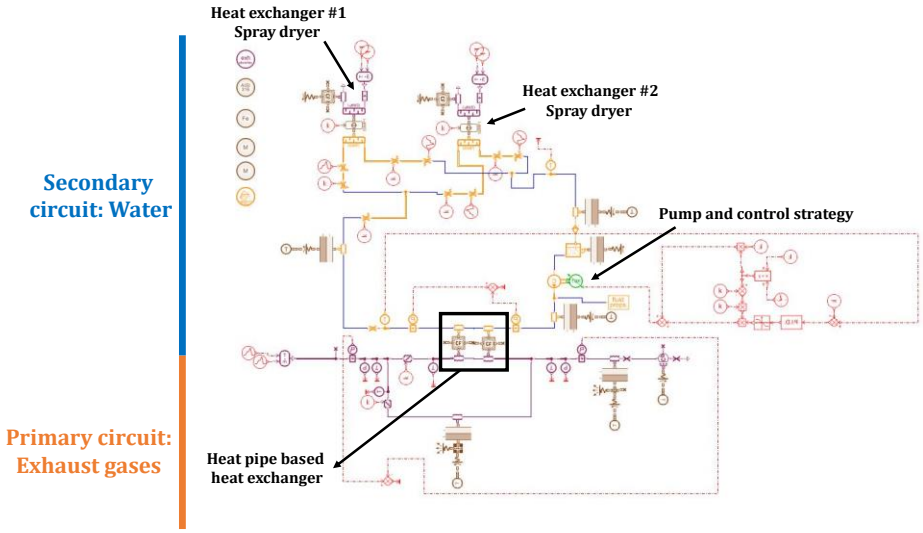

Figure 3 – Layout of the numerical model of the whole heat recovery system

The focus of this analysis is the investigation of the whole thermal performance of the heat recovery circuit, as well as the evaluation of the effectiveness of the control strategy of the system in order to maintain the desired operating parameters under different working conditions, i.e. different flow rates and temperatures of the exhaust gases.
In the model, particular care is devoted to the heat loss modelling of the exhaust and the water along the primary and secondary circuit respectively; furthermore, specific models for the water pump and for the two heat exchangers that transfer the heat recovered by the water to the spray dryer are developed in the model.
In the following, a description of the model adopted for the components displayed in Figure 3 is presented.

Thermal losses of the primary and secondary side
As already mentioned, the numerical model developed accounts for the thermal losses in the exhaust and water circuit; the thermal exchange is considered between the fluid and an external ambient with an imposed temperature of 25 °C.
The heat transfer between the fluid and the external ambient is composed by three contribution: convection between the fluid and the wall, conduction within the wall of the material and the external convection between the material and the external ambient.
The first contribution, the convective heat exchange "qConvection" between the fluid, i.e. exhaust gases or water, and the material, i.e. wall of the pipe, is computed according to the following equation:

$$qConvection = h_{conv} * area_{conv} \ (t3 - t2) \ Eq.1$$

Where $area_{conv}$ is the convective heat exchange area [m^2], t3 and t2 are respectively the temperature of the gases and the wall [K].
The heat transfer coefficient h_{conv} is calculated as:

$$h_{conv} = \frac{Nu * \lambda}{dh} \ Eq.2$$

Where Nu is the Nusselt number, λ is the thermal conductivity of the fluid [W/m*K] and dh is the hydraulic diameter [m].
In the case analysed, both the exhaust and the water piping are insulated; thus, the heat transferred by the conduction phenomenon within the walls of the pipes can be retrieved according from:

$$qConduction = \frac{t_{layer\ N} - t_{layer\ N+1}}{\frac{d_N}{Area * \lambda_N} + \frac{d_{N+1}}{Area * \lambda_{N+1}}}\ Eq.3$$

where $t_{layer\ N}$ is the temperature of material layer N, d_N is the distance between temperature point of material layer N and temperature point of material layer N+1, Area is the heat exchange area, λ_N is the thermal conductivity of material layer N.
The same definitions apply for the properties of material N+1.

Finally, the last contribution is the heat exchange between the piping walls and the external environment which is calculated according the Equation N.1. The external ambient temperature is set equal to 25 °C and the heat transfer coefficient is 6 W/m^{2}K, which is a standard coefficient of natural convection.

Water circuit
The secondary flow is pumped into the HPHE by means of a thermal-hydraulic centrifugal pump. The delta pressure of the fluid passing through the pump is calculated using affinity laws. The fluid temperature at the pump outlet is computed from the temperature at the pump inlet and the energy provided (with an overall efficiency) by the pump to the water.
The characteristic curves (volumetric flow rate-pump head) have been implemented in the software for different velocities.

The mass flow rate at the suction of the pump is calculated so that the output pressure (high pressure) reaches the following value

$$p_{out}=p_{in}+\Delta p\ \ Eq.4$$

where p_{in} is the input pressure (low pressure) and Δp is the pressure difference. The pressure difference into the pump is interpolated thanks to the reference data.
The power P_{mech} provided by the pump to the fluid is as follows:

$$P_{mech}=Q\cdot\Delta p\ f_{eff}\ Eq.5$$

$$0 \leq f_{eff} \leq 1\ Eq.6$$

where Q is the volumetric flow rate, Δp the pressure difference and f_{eff} the global efficiency of the pump.
The super-heated thermal fluid flows in the secondary piping toward the intermediate heat exchangers that transfer the recovered heat to the air required by the spray-dryer process; the two heat exchangers are placed in parallel and they are designed to transfer 490 kW and 180 kW respectively to the air required by the spraydryer process.
In the numerical model, the heat exchangers are modelled according to the efficiency-NTU method.
A warm fluid with mass flow rate dm_{hot} [kg/s] enters the heat exchanger at temperature $T_{hot,in}$ [degC] and goes out the heat exchanger at temperature $T_{hot,out}$ [degC]. Meanwhile a cold fluid with mass flow

rate dm_{cold} [kg/s] enters the heat exchanger at temperature $T_{cold,in}$ [degC] and goes out the heat exchanger at temperature $T_{cold,out}$ [degC].
The heat transfer rate between the cold fluid and the hot fluid cannot exceed a maximum value Q_{max}. This value is given by:

$$Q_{max}=C_{min}\cdot(T_{hot,in}-T_{cold,in}) \quad Eq.7$$

where C_{min} is the minimum heat flow rate capacity written as:

$$C_{min}=\min(|dm_{hot}|\cdot Cp_{hot},|dm_{cold}\cdot Cp_{cold}) \quad Eq.8$$

The efficiency-NTU method states that the heat flux can be written as:

$$Q=\epsilon\cdot Q_{max} \quad Eq.9$$

where ε is the efficiency or thermal effectiveness of the heat exchanger.

This thermal effectiveness can be written as a function of the number of transfer unit NTU and the flow-stream capacity ratio Cr:

$$\epsilon=f(NTU,Cr) \quad Eq.10$$

NTU and Cr are defined as:

$$NTU= UA / C_{min} \quad Eq.11$$

$$Cr= C_{min} / C_{max} \quad Eq.12$$

where:

$$U * A = \frac{1}{R_{hot} + R_{wall} + R_{cold}} \quad Eq.13$$

$$C_{max}=\max(|dm_{hot}|\cdot Cp_{hot},|dm_{cold}|\cdot Cp_{cold}) \quad Eq.14$$

R_{hot}, R_{wall} and R_{cold} are the thermal resistance in K/W at hot fluid level, wall level and cold fluid level respectively.

Control strategy
In the numerical model, a temperature sensor is placed at the Condenser Outlet in order to measure the temperature of the water flow; the pump varies its rotational velocity from the minimum of 1800 rpm to the maximum of 3000 rpm to maintain the water stream at the desired value, i.e. 165°C.
Thus, if the thermal power available in the exhaust stream is higher than the designed value, the pump increases the water flow rate in order to avoid the overheating of the water flow; in the event that this control strategy is inadequate for keeping the temperature at the desired value, the bypass of the HPHE in the primary side, i.e. exhaust, is partially opened to decrease the thermal power available in the gases.
Conversely, a decrease in the temperature or the flow rate of the exhaust gases at the inlet of Evaporator with the respect to the designed values could determine a decrease of the temperature of the exhaust at

the outlet of the system; this condition must be avoided due to the acid condensate that could occur in the exhaust.
As a consequence, in this scenario the inverter decreases the speed of the pump to reduce the water flow rate; when the decrease of the thermal power available in the exhaust is significant, the control strategy activates a bypass of the intermediate heat exchangers in order to transfer less thermal power to the spray dryer. Thus, the heat recovered in the HPHE by the water will decrease determining a rise in the temperatures' values.

Experimental-numerical validation of the flue gases heat losses
As mentioned above, the first case is the simulation considering only the exhaust gases circuit, i.e. no heat recovery is considered in the simulation, in order to compare the numerical results with the experimental data; this simulation is useful to determine the gap between the experimental and numerical thermal losses along the exhaust piping.
The experimental temperature and flow rate measured by the sensors at the manifold, see the sensors location in Figure 2, are implemented in the numerical model as input parameters for the exhaust gases source.
The following Figure shows the experimental values simulated over a period of approximately 2 days; the temperature detected at the manifold varies from a minimum of 210 °C to a maximum of 260 °C while the flow rate have been normalized on the basis of its maximum value according to the following equation:

$$\text{FlowRate} = (\text{FlowRate} / \text{FlowRate Max}) * 100 \quad \textit{Eq.15}$$

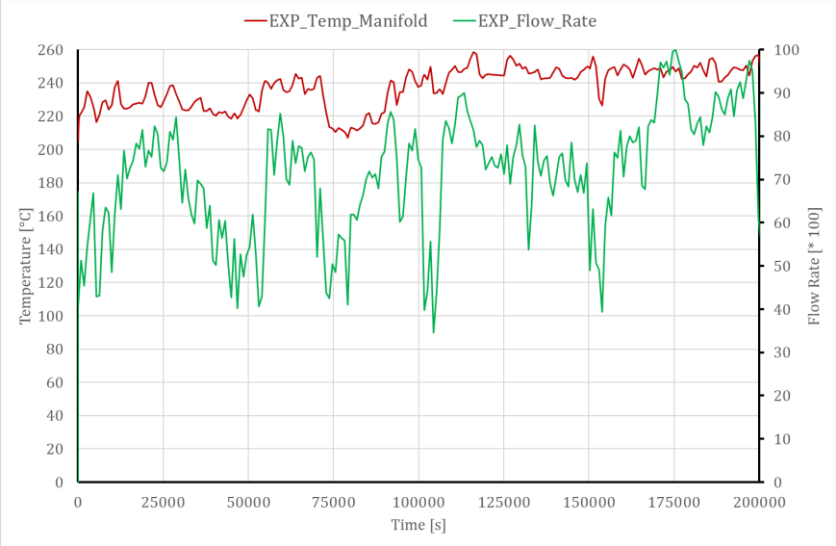

Figure 4 - Experimental temperature and flow rate of the exhaust at the manifold implemented in the numerical model as input data.
Figure 5 shows the comparison between the numerical and calculated temperature of the gases before the main stack (where the heat pipe based heat exchanger will be installed).
The agreement between the numerical results and the experimental measurements is satisfactory; thus, the thermal losses of the exhaust gases along the piping is correctly predicted.

Indeed, the time-dependent temperature curves are aligned, and the difference is approximately 4-5 °C; a maximum difference of 7 °C can be noticed at approximately 75000 seconds.

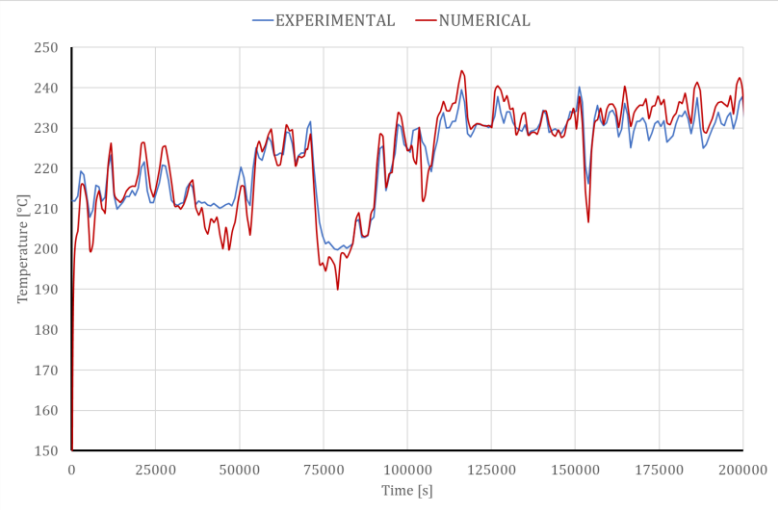

Figure 5 – Experimental and numerical temperature of the before the main stack

Numerical-theoretical validation of the entire heat recovery system

In the second simulation the heat recovery system is accounted in the simulation; particularly, the heat pipe based heat exchanger and the closed loop heat transfer fluid circuit presented in the previous paragraph are included in the numerical model.

The simulation has been carried out with the designed temperature and flow rate at the inlet of the exhaust piping and with the designed rotational speed of the pump: the exhaust temperature is equal to 245°C while the pump rotational speed is equal to 2520 rpm. The initial temperatures of the materials components and of the water flow is 20 °C.

This simulation determines the deviation between the numerical results and the operating parameters of the designed heat recovery system shown in Table 2, which are determined by theoretical correlations.

Figure 6 displays the main numerical operating parameters of the system: the temperature of the exhaust gases at the outlet of the HPHE and the inlet and outlet temperatures of the water from the HPHE and the thermal power recovered by the heat exchanger.

The warm-up phase of the water flow can be noticed at the beginning of the simulation: the water takes approximately 10000 seconds to reach its steady value of 115.4°C.

The water temperature at the outlet of the heat exchanger stabilizes at 166.7 °C while the numerical temperature of the exhaust before flowing to the atmosphere is 155.5 °C.

These numerical results are very close to the designed parameters of the system reported in Table 2.

The numerical thermal power recovered by the HPHE is reported in Figure 6 and it is equal to 716850 W; the error with the designed recovered power, i.e. 700 kW, is the 2.4 %.

Thus, the numerical model is able to reproduce the designed heat recovery system operating parameters determined by theoretical correlations.

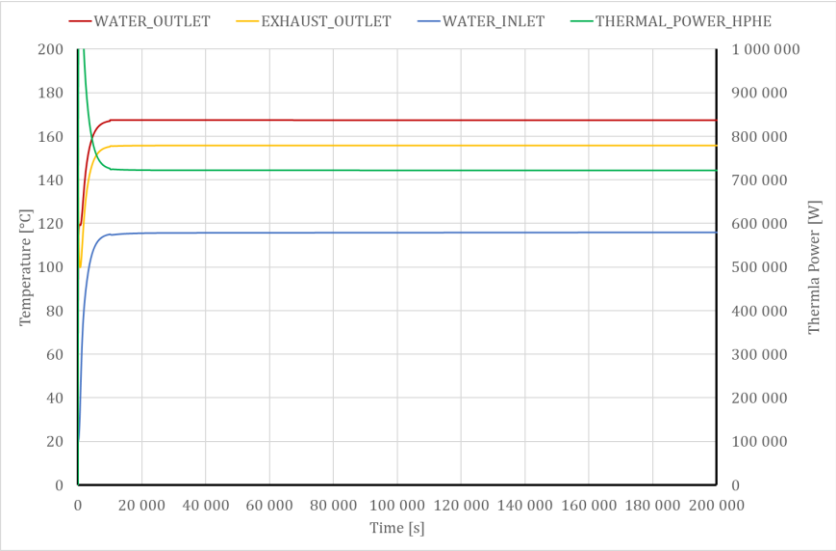

Figure 6 –Numerical temperature of the exhaust at the outlet of the HPHE (yellow line) and of the water at the inlet (blue line) and outlet (red line) of the HPHE. Thermal Power recovered by the HPHE (green line).

4 Control strategy sensitivity analysis

Once the numerical model has been validated against experimental data and theoretical correlations, the 0D/1D model has been used to simulate different working points of the heat recovery system under variable boundary conditions.

Different simulations have been carried out to investigate the thermal performance of the system in situation that could occur during the real working conditions.

Case A

In this scenario, the inputs of the exhaust gases have been kept equal to their designed value: 245 °C and 1 (non dimensional value for the flow rate). The pump rotational speed is maintained constant to the designed value of 2520 rpm.

The influence of two parameters have been analysed on the thermal behaviour of the system: the opening of the bypass of the Evaporator of the HPHE and a reduction of the flow rate of the spray-dryer air (the secondary flows that recover the heat in the intermediate heat exchangers).

In both the intermediate heat exchangers, a reduction in the air flow rate has been investigated: the air flow rate has been decreased from the nominal value of 100% (designed working condition) up to the 10% reducing the flow rate of a 10% step every simulation.

The following Table summarizes the simulations carried out varying the air flow rate in the intermediate heat exchangers.

Table 3. Simulated scenarios varying the flow rate of the intermediate heat exchangers

Simulation #N	Flow Rate Intermediate HE#1	Flow Rate Intermediate HE#2
1	100	100
2	90	90
3	80	80
4	70	70
5	60	60
6	50	50
7	40	40
8	30	30
9	20	20
10	10	10

The influence of the opening of the bypass of the HPHE Evaporator has been investigated for every simulation reported in Table 3. In particular, different by pass angle have been considered starting from the bypass valve angle equal to 0 (completely closed) up to 90 (completely opened) varying the opening angle of 10 degrees every simulation.
Thus, considering the simulation carried out varying the flow rate of the intermediate heat exchangers and the influence of the bypass opening valve, a matrix of 100 simulations is determined.

Figure 7, Figure 8 and Figure 9 show the numerical results of the simulations' matrix carried out for this analysis; in particular, the temperature of the exhaust at the outlet of the HPHE and the temperature of the water stream at inlet and outlet of the Condenser are presented.
For each variable analysed an operating 3D map and a table summarizing the numerical results have been obtained to determine the working points of the heat recovery system considering the different openings of the bypass valve and the air flow rates in the intermediate heat exchangers simulated.
The temperature of the flue gases is shown in Figure 7. As it can be noticed, in the designed condition (flow rate spray-dryer 100% and bypass closed) the temperature is 155 °C; thus, increasing the opening of the bypass valve a greater amount of the exhaust flow rate flows in the bypass and the heat recovery in the heat exchanger decreases. No heat recovery takes place when the bypass valve is completely opened, i.e. 90 degrees, because the exhaust completely bypasses the heat exchanger.
Furthermore, the increase in the exhaust gases temperature is determined also by the decrease in the air flow rate in the intermediate heat exchangers; a maximum temperature of 228 °C can be reached when the air flow rate in the intermediate heat exchangers is the 10% of the designed value.
A similar behaviour can be noticed for the water temperature at the inlet (Figure 8) and at the outlet (Figure 9) of the Condenser of the HPHE.
Indeed, the temperature is approximately 115 °C and 167 °C at the inlet and outlet respectively in the designed working condition, i.e. 100% of the air flow rate in the intermediate heat exchanger and bypass completely closed. The temperature of the water (both at the inlet and outlet) decreases opening the bypass valve angle; indeed, a lower amount of thermal energy can be recovered in the HPHE.
If the air flow rate in the intermediate heat exchangers decreases, the temperatures of the water increase; it is necessary the opening of the bypass to keep the water temperatures in the desired range.

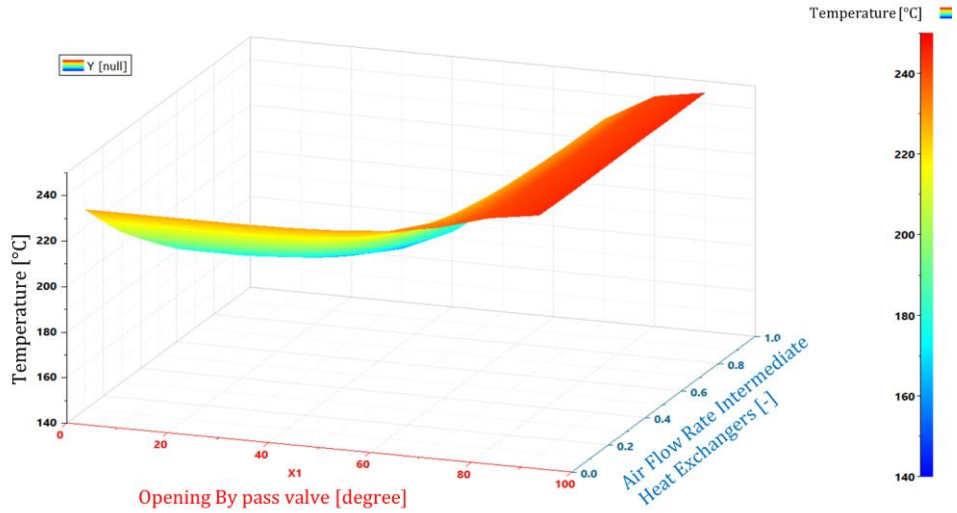

Air Flow Rate Intermediate Heat Exchangers	Opening bypass valve angle [degree]									
	0	10	20	30	40	50	60	70	80	90
100%	155.6	156.1	158.4	163.5	173.1	188.8	209.4	228.9	241.2	244.8
90%	161.2	161.7	163.7	168.2	176.8	191.1	210.3	229.1	241.2	244.8
80%	167.3	167.7	169.5	173.4	180.9	193.6	211.3	229.3	241.2	244.8
70%	173.9	174.2	175.7	179	185.4	196.6	212.6	229.6	241.2	244.8
60%	181	181.3	182.5	185.2	190.5	200	214.2	229.9	241.2	244.8
50%	188.8	189	190	192	196.2	204	216	230.4	241.3	244.8
40%	197.3	197.5	198	199.5	202.7	209.5	218.4	231	241.4	244.8
30%	206	206.6	207	208	210	214	221.4	231.9	241.4	244.8
20%	216.5	216.7	217	217.4	218.6	221	225.3	233	241.4	244.8
10%	227.9	227.8	227.9	228.1	228.5	229.5	231.3	235.3	241.5	244.8

Figure 7 –Numerical temperature of the exhaust at the outlet of the HPHE varying the air flow rate in the intermediate heat exchangers (spray dryer) and the opening of the bypass valve in the exhaust flow

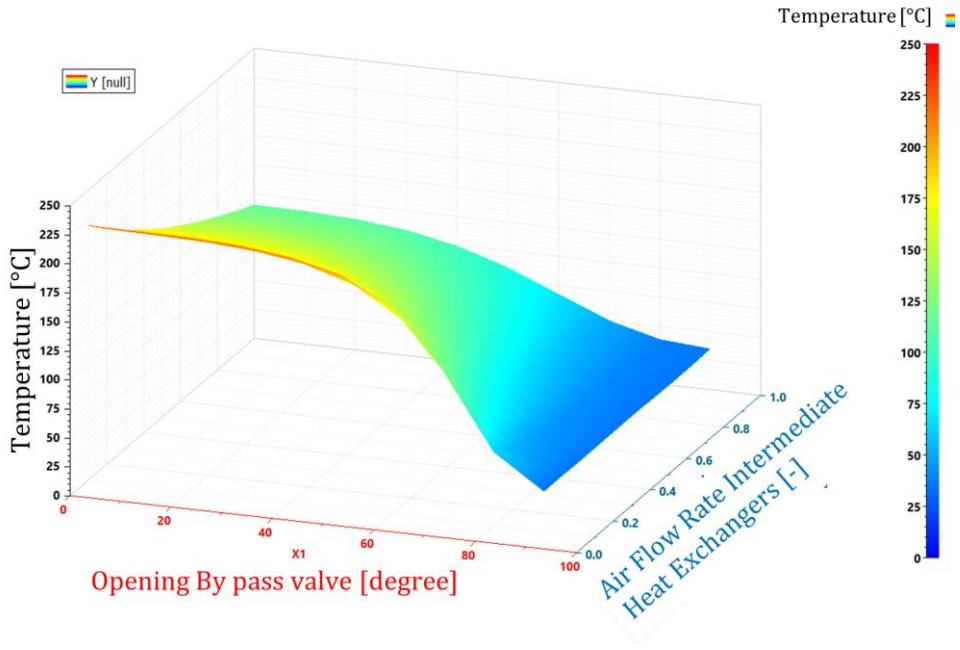

Air Flow Rate Intermediate Heat	Opening bypass valve angle [degree]									
	0	10	20	30	40	50	60	70	80	90
100%	114,7	114,2	112,2	107,8	99,5	85,8	67,5	49,8	38,4	35,08
90%	122,8	122	120,3	115,7	107	92,3	72,2	52	38,8	34,8
80%	131,6	131	129	124,3	115,2	99,6	77,7	54,9	39,5	34,8
70%	141,1	140,6	138,5	133,7	124,3	108	84,2	58,4	40,4	34,8
60%	151,4	150,9	148,8	144	134,6	117,7	92	62,7	41,6	34,8
50%	162,6	162	160,1	155,5	146,1	128,9	101,5	68,5	43,1	34,8
40%	174,9	174,4	172,2	168,2	159,2	142,1	113,4	76,1	45,3	34,8
30%	188,4	187,9	186,2	182,4	174,2	158	128,5	86,8	48,4	34,8
20%	203	202,8	201,5	198,3	191,5	177,2	149	102,9	53,7	34,8
10%	219	219	218,5	216,3	211	200,9	177,8	129	63,9	34,8

Figure 8 –Numerical temperature of the water at the inlet of the HPHE varying the air flow rate in the intermediate heat exchangers (spray dryer) and the opening of the bypass valve in the exhaust flow

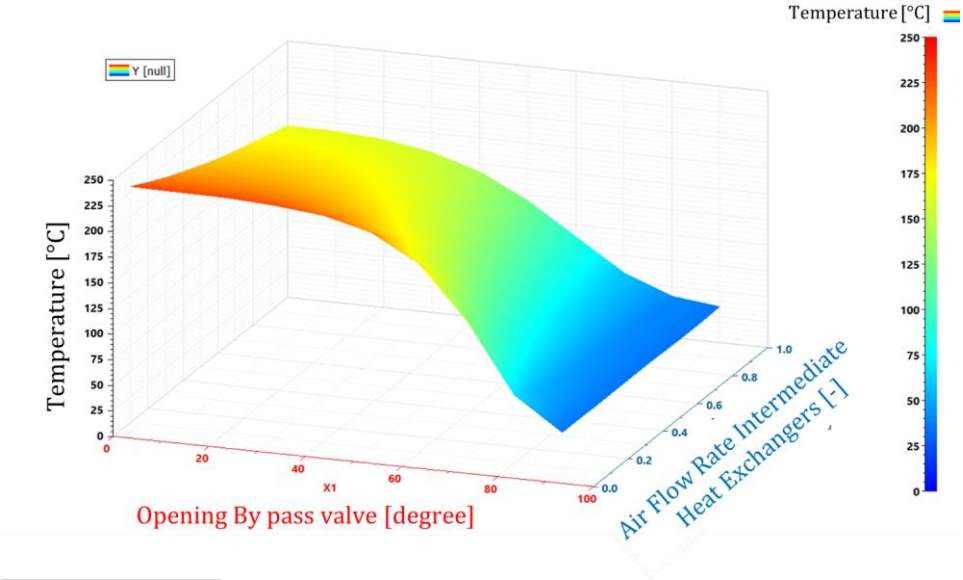

Air Flow Rate Intermediate Heat Exchangers	Opening bypass valve angle [degree]									
	0	10	20	30	40	50	60	70	80	90
100%	167.6	166.8	163.5	156	142	119	88.5	59	40.8	35.1
90%	172.6	171.7	168.5	161.2	147.3	124.2	92.6	61.4	41	34.9
80%	177.9	177	174	166.9	153.2	130	97.5	64	41.7	34.8
70%	183.6	182.8	180	173	159.8	136.7	103.2	67.4	42.6	34.8
60%	189.8	189	186.2	179.8	167.1	144.4	110.2	71.6	43.8	34.8
50%	196.5	195.8	193.3	187.3	175.3	153.4	118.6	77	45.3	34.8
40%	203.8	203.2	201	195.6	184.7	163.9	129.2	84.3	47.3	34.8
30%	211.8	211	209.2	204.9	195.3	176.5	142.8	94.5	50.5	34.8
20%	220.6	220	218.7	215.2	207.5	191.8	160.5	109.2	55.8	34.8
10%	230.3	230	229	226.7	221.7	210.7	185	134.6	65.7	34.8

Figure 9 –Numerical temperature of the water at the outlet of the HPHE varying the air flow rate in the intermediate heat exchangers (spray dryer) and the opening of the bypass valve in the exhaust flow

As already mentioned, the temperature at the outlet of the HPHE is one of the main parameters that need to be monitored in order to avoid the acid condensate of the exhaust gases; the opening of the flue gases bypass will be used to maintain the temperature in the desired range.
Thus, the matrix of the simulations carried out has been used to determine the exhaust gases temperature increase per unit time [°C/s]; this calculated value is fundamental for the tuning of the control strategy in order to open the bypass valve at the right angle when a perturbation occur.
Figure 10 shows the temperature gain [°C/s] (y-axis) for the flue gases at the HPHE outlet per each spray-drier mass flow rate and per each bypass valve opening angle simulated (x-axis).
Analysing the curve at a random spraydryer flow rate, it is clearly visible that, as expected, the temperature gain increases with the increase of the bypass valve opening; for instance, looking at the 100% air flow rate curve, the temperature gain increases from 0.0003 °C/s at 10 degrees bypass valve

opening up to 0.23 °C/s when the bypass is completely opened. For the same curve, when the bypass is opened at 20 degrees, the gain is 0.006 °C/s which means approximately 3.6 °C in ten minutes.
In addition to this, for a certain bypass valve opening, the temperature gain increases with the decrease of the air flow rate at the intermediate heat exchangers; indeed, less thermal energy is exploited when the air flowrate decreases. Thus, the water stream flows at the inlet of the Condenser at a higher temperature, recovering less thermal energy in the HPHE Condenser inlet and determining an increase of the exhaust at the outlet of the Evaporator.

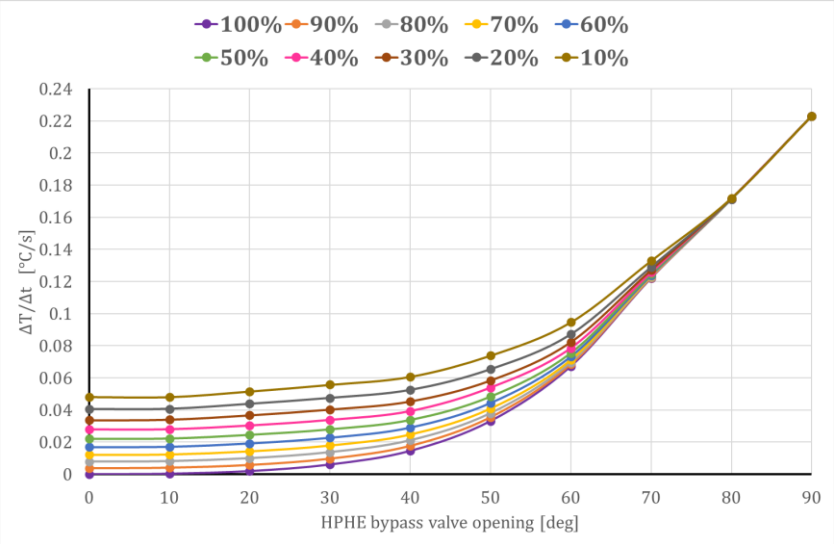

Figure 10- Exhaust temperature gain per unit time [°C/s] under different bypass valve openings and spray-dryer flow rates

Case B

Finally, the control strategy has been tested in two conditions that simulate different perturbations that could occur in the real system: an excess and a decrease of thermal energy available in the exhaust gases.
The first simulation is related to a higher energy content in the exhaust: in particular, data characterized by a higher temperature and flow rate than the designed value are implemented as input to the numerical model. Finally, the second simulation concerns with a temperature and a flow rate in the exhaust lower than the designed value.
Figure 11 shows the temperature and flow rate of the two perturbations simulated; the exhaust flow rate is normalized to the designed value in both cases.
After a simulation time of 30000 seconds where the input parameters are kept constant to the design values in both cases, the perturbations occur: in Figure 11.a) (simulation with higher energy content) the temperature and the flow rate of the exhaust reach the 260°C and the 120 % respectively while in the simulation with the less energy content the temperature and flow rate decrease up to 210 °C and 76 %, see Figure 11.b).
In these simulations the control strategy is activated; thus, the speed of the pump is regulated to maintain the water temperature at the Condenser outlet at 165 °C.

If the variation of the water flow rate is not sufficient, a partial bypass of the Evaporator will be operated in case of excess of thermal power in the exhaust while the bypass of one intermediate heat exchanger will be performed in the second simulation, i.e. decrease of thermal power in the flue gases.

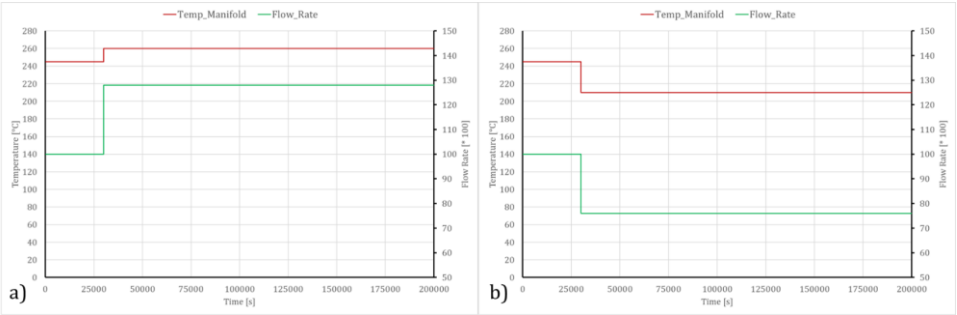

Figure 11 - Experimental temperature and flow rate of the exhaust at the manifold implemented in the numerical model as input for the excess of thermal power (a) and the decrease of thermal power (b)

In the following paragraph, the results of the two perturbations are reported.

Excess of thermal power in the flue gases

Figure 12 shows the numerical results of the simulation with the excess of thermal power in the exhaust.

The temperatures of two streams and the rotational speed of the pump are shown in figure 12.a). When the source of the exhaust gases are in the designed condition (245 °C and 100 % of flow rate) the temperatures stabilize at the nominal conditions: 155 °C for the exhaust temperature at the outlet of the HPHE Evaporator, 115 °C and 165°C for the water temperature at the inlet and outlet of the HPHE Condenser respectively. The nominal conditions are reached also for the pump rotational speed, see Figure 12.a, and thermal power recovered, see Figure 12.b).

A major energy content in the exhaust (starting from 30000 seconds) determines an increased thermal power recovered in the HPHE that is approximately 14% more with the respect to the thermal power recovered in the nominal conditions. Thus, an increase of the characteristic temperatures can be noticed; indeed, the flue gases temperature before exiting to the atmosphere is 181 °C while the water stream temperatures registered are 135 °C and 186 °C at the inlet and outlet of the Condenser respectively.

Figure 12.a) shows that the pump accelerates up to 3000 rpm when the perturbation occurs but the increased water flow rate in not sufficient to maintain the temperature of the water at the desired temperature: 165°C.

Thus, the opening of the bypass valve is operated at 50000 seconds to reduce the energy content in the exhaust gases; the bypass valve opening angle is 40 degrees.

The thermal power recovered by the HPHE shown in Figure 12.b) decreases up to the nominal value, i.e. 700 kW and the water temperature at the outlet of the Condenser stabilizes at 165 °C.

The opening of the bypass valve generates an increase of the exhaust temperature, i.e. 195 °C; the delta temperature gained by the exhaust is approximately 15°C in 20 minutes, which is very close to the rate shown in Figure 10 for the same valve opening.

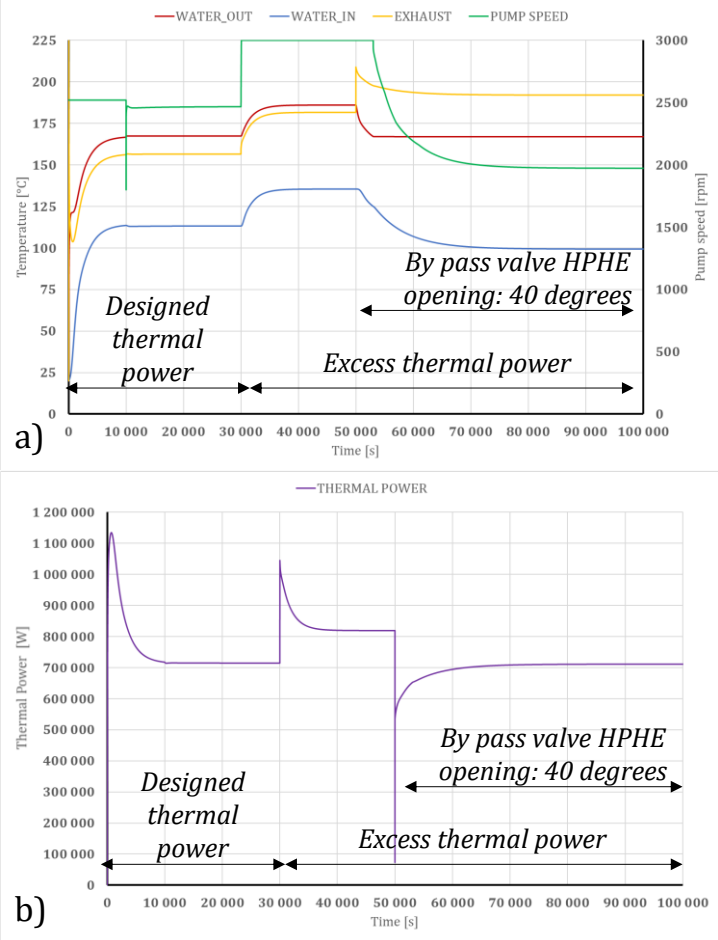

Figure 12 – Numerical results of the excess of thermal power in the exhaust. (a) Numerical temperatures of the exhaust at the outlet of the HPHE, numerical temperatures of the water at the inlet and outlet of the HPHE and rotational speed of the pump. (b) Thermal power recovered by the HPHE.

Decrease of thermal power in the flue gases

Finally, the results of the perturbation with the lower energy content in the exhaust with the respect to the nominal condition are shown.

The thermal behaviour of the system is the same as the one shown in the previous paragraph when the designed conditions are simulated, up to 30000 seconds. The decreased of the energy content in the exhaust, starting at 30000 seconds, determines a lower thermal energy recovered by the HPHE: 550 kW with the respect to the 700 kW recovered in the nominal condition, see Figure 13.b).

The control strategy slows down the pump's speed when the perturbation is registered, i.e. 30000 seconds, to decrease the water flow rate in the Condenser but it is not sufficient to maintain the water

temperature at 165 °C; indeed, the water stabilizes at 137 °C and 80 °C at the inlet and outlet respectively while the flue gases temperature is 120 °C, see Figure 13.a).
The solution to increase the characteristic temperatures is the bypass of the intermediate heat exchanger to exploit less thermal energy in the spray-dryer.
Thus, at 50000 seconds the bypass of the main heat exchanger is performed; as it can be seen from Figure 13.a), the temperatures rise. The speed of the pump increases up to 3000 rpm to keep the 165 °C.

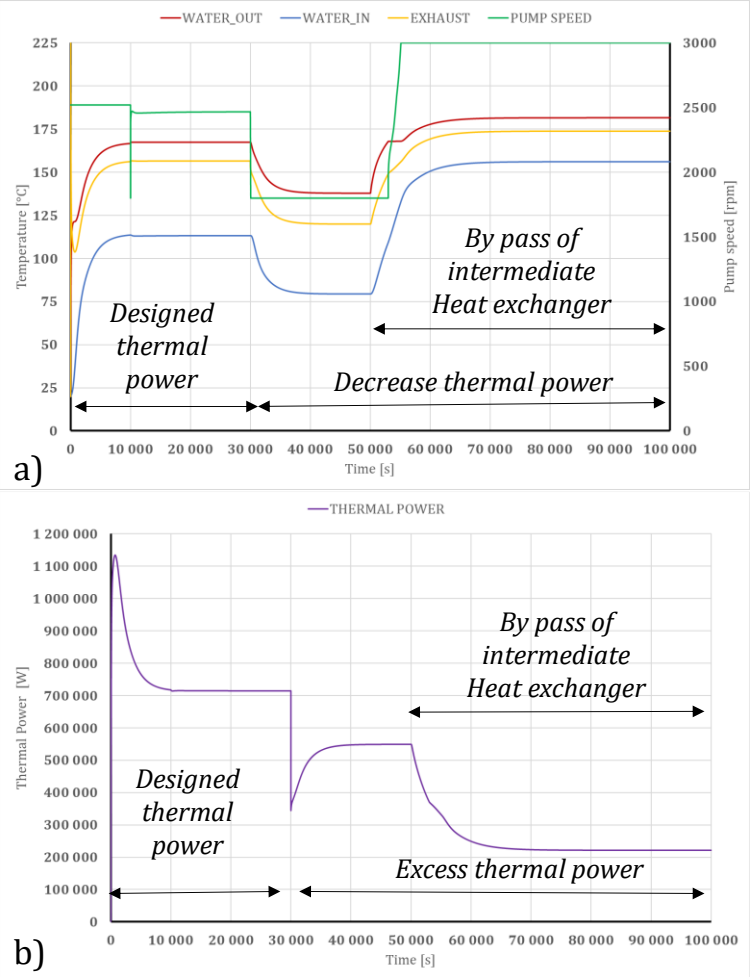

Figure 13 – Numerical results of the decrease of thermal power in the exhaust.
(a) Numerical temperatures of the exhaust at the outlet of the HPHE, numerical temperatures of the water at the inlet and outlet of the HPHE and rotational speed of the pump. (b) Thermal power recovered by the HPHE.

CONCLUSIONS

In this paper, the energy efficiency enhancement due to the heat recovery from the flue gases of two ceramic furnaces has been evaluated. The application of a heat-pipe based heat exchanger to improve the energy efficiency and to reduce the environmental impact of a ceramic process is investigated.
In the study, a lumped and distributed numerical model of the exhaust piping from the outlet of the furnaces to the main stack has been constructed and validated against experimental data.
The agreement between the calculations and the measurement resulted satisfactory when investigating the thermal losses along the flue gases piping.
Afterward, the numerical model of the entire heat recovery system has developed to investigate the thermal performance of the system and to tune the control strategy of the heat recovery circuit.
Indeed, the 0D/1D model accounts for the main components of the circuit: the heat pipe based heat exchanger and the heat transfer fluid closed loop circuit with specific models for the pump and the heat exchangers that exploit the energy recovered in the heat sink.
The results of the proposed numerical model are validated against theoretical correlations under the nominal working condition designed for the system.
3D operating maps are determined to investigate the influence of the variation of the spray-dryer flow rate and of the opening of the bypass valve on the thermal performance of the heat recovery system under the nominal working conditions, i.e. designed exhaust temperature and flowrate.
Finally, the control strategy behaviour is investigated under two different perturbations: excess and decrease of thermal energy content in the exhaust.
The numerical analysis demonstrated that it is necessary the opening of the bypass valve of 40 degrees when the maximum spike in the exhaust flow rate and temperature is registered while a bypass of the main heat exchanger is necessary when the energy content of the exhaust is the minimum.

ACKNOWLEDGEMENTS

The present work is part of HEAT PIPE TECHNOLOGY FOR THERMAL ENERGY RECOVERY IN INDUSTRIAL APPLICATIONS — ETEKINA project. The project has received funding from the European Union's Horizon 2020 research and innovation programme under grant agreement N° 768772.

REFERENCES

[1] Egilegor, B., Jouhara, H., Zuazua, J., Al-Mansour, F., Plesnik, K., Montorsi, L., & Manzini, L. (2020). ETEKINA: analysis of the potential for waste heat recovery in three sectors: aluminium low pressure die casting, steel sector and ceramic tiles manufacturing sector. International Journal of Thermofluids, 1 (2020), 100002, https://doi.org/10.1016/j.ijft.2019.100002
[2] Confindustria Ceramica Report.
[3] Jouhara, H., Khordehgah, N., Almahmoud, S., Delpech, B., Chauhan, A., & Tassou, S. A. (2018). Waste heat recovery technologies and applications. Thermal Science and Engineering Progress, 6, 268-289., https://doi.org/10.1016/j.tsep.2018.04.017
[4] Daniel Brough , Hussam Jouhara , The Aluminium Industry: A Review on State-of-the-Art Technologies, Environmental Impacts and Possibilities for Waste Heat Recovery, International Journal of Thermofluids (2020), https://doi.org/10.1016/j.ijft.2019.100007
[5] European Commission, Reference Document in the Ceramic Manufacturing Industry, 2007.
[6] Mezquita, A., Boix, J., Monfort, E., & Mallol, G. (2014). Energy saving in ceramic tile kilns: Cooling gas heat recovery. Applied Thermal Engineering, 65 (1-2), 102-110. https://doi.org/10.1016/j.applthermaleng.2014.01.002
[7] Agrafiotis, C., & Tsoutsos, T. (2001). Energy saving technologies in the European ceramic sector: a systematic review. Applied thermal engineering, 21(12), 1231-1249. https://doi.org/10.1016/S1359-4311(01)00006-0

[8] Peris, B., Navarro-Esbrí, J., Molés, F., & Mota-Babiloni, A. (2015). Experimental study of an ORC (organic Rankine cycle) for low grade waste heat recovery in a ceramic industry. Energy, 85, 534-542. https://doi.org/10.1016/j.energy.2015.03.065
[9] Milani, M., Montorsi, L., Stefani, M., Saponelli, R., & Lizzano, M. (2017). Numerical analysis of an entire ceramic kiln under actual operating conditions for the energy efficiency improvement. Journal of environmental management, 203, 1026-1037. https://doi.org/10.1016/j.jenvman.2017.03.076.
[10] Milani, M., Montorsi, L., Storchi, G., Venturelli, M., Angeli, D., Leonforte, A., Castagnetti, D., Sorrentino, A. Experimental and Numerical Analysis of a Liquid Aluminium Injector for an Al-H2O based Hydrogen Production System. International Journal of Thermofluids (2020), 100018 https://doi.org/10.1016/j.ijft.2020.100018
[11] Vega, A-M. Nuñez, B. Sturm, and W. Hofacker. "Simulation of the convective drying process with automatic control of surface temperature." Journal of Food Engineering 170 (2016): 16-23. https://doi.org/10.1016/j.jfoodeng.2015.08.033
[12] Bunyawanichakul, P., Walker, G. J., Sargison, J. E., & Doe, P. E. (2007). Modelling and simulation of paddy grain (rice) drying in a simple pneumatic dryer. Biosystems engineering, 96(3), 335-344. https://doi.org/10.1016/j.biosystemseng.2006.11.004
[13] Ramadan, M., Ali, S., Bazzi, H., & Khaled, M. (2017). New hybrid system combining TEG, condenser hot air and exhaust airflow of all-air HVAC systems. Case studies in thermal engineering, 10, 154-160. https://doi.org/10.1016/j.csite.2017.05.007
[14] Luo, Y., Zhang, L., Liu, Z., Wu, J., Zhang, Y., & Wu, Z. (2018). Numerical evaluation on energy saving potential of a solar photovoltaic thermoelectric radiant wall system in cooling dominant climates. Energy, 142, 384-399. https://doi.org/10.1016/j.energy.2017.10.050
[15] Brough, D., Mezquita, A., Ferrer, S., Segarra, C., Chauhan, A., Almahmoud, S., Khordehgah, N., Ahmad, L., Middleton, D., Sewell, H.I., Jouhara, H. (2020). An experimental study and computational validation of waste heat recovery from a lab scale ceramic kiln using a vertical multi-pass heat pipe heat exchanger. Energy, 208, 118325. https://doi.org/10.1016/j.energy.2020.118325
[16] Milani, M., Montorsi, L., & Terzi, S. (2017). Numerical analysis of the heat recovery efficiency for the post-combustion flue gas treatment in a coffee roaster plant. Energy, 141, 729-743. https://doi.org/10.1016/j.energy.2017.09.098
[17] Delpech, B., Milani, M., Montorsi, L., Boscardin, D., Chauhan, A., Almahmoud, S., Axcell B., Jouhara, H. (2018). Energy efficiency enhancement and waste heat recovery in industrial processes by means of the heat pipe technology: Case of the ceramic industry. Energy, 158, 656-665. https://doi.org/10.1016/j.energy.2018.06.041
[18] Gómez, H. O., Calleja, M. C., Fernández, L. A., Kiedrzyńska, A., & Lewtak, R. (2019). Application of the CFD simulation to the evaluation of natural gas replacement by syngas in burners of the ceramic sector. Energy, 185, 15-27. https://doi.org/10.1016/j.energy.2019.06.064
[19] Ershadi, H., & Karimipour, A. (2018). Present a multi-criteria modeling and optimization (energy, economic and environmental) approach of industrial combined cooling heating and power (CCHP) generation systems using the genetic algorithm, case study: a tile factory. Energy, 149, 286-295. https://doi.org/10.1016/j.energy.2018.02.034
[20] Milani, M., Montorsi, L., Venturelli, M., Tiscar, J. M., & García-Ten, J. (2019). A numerical approach for the combined analysis of the dynamic thermal behaviour of an entire ceramic roller kiln and the stress formation in the tiles. Energy, 177, 543-553. https://doi.org/10.1016/j.energy.2019.04.037
[21] Heat pipe technology for thermal energy recovery in industrial applications (ETEKINA), Research and Innovation Action, European Union. Grant agreement N° 768772.
[22] Simcenter AMESim 2019 User Guide